temperature, the CO_2-rich phase L_2, which forms second upon pressurization of the initial L–V system with CO_2, appears below the L_1 phase in the cell. Above the inversion temperature, the L_2 phase forms above the L_1 phase. In the CO_2–butylbenzene system, the L_2 phase is denser than the L_1 phase. Phase inversions have been previously observed by the authors in L_1–L_2–V systems, specifically for the ternary system CO_2–*n*-butylbenzene–n-eicosane (*8*), as the CO_2-free mole fraction of *n*-butylbenzene in *n*-eicosane in L_1 reached 0.79.

The melting point of *n*-butylbenzene is low enough that the solid crystals at the *Q* point in Table III are CO_2 (labeled S_2). The solid crystals at the *Q* point in Table IV are *trans*-decalin (labeled S_1).

The standard deviations of the raw data from the smoothed values of composition and molar volume in Tables I and II are ±0.004 and ±0.7 mL/g-mol, respectively, while, for the L_1–L_2–V systems in Tables III and IV, for pressure, compositions, and molar volumes, they are ±0.15 atm, ±0.004, and ±0.6 mL/g-mol, respectively. In the case of Tables I and II, the "flatness" of the data with respect to pressure at high pressures, for temperatures below the critical temperature of CO_2, increases the standard deviations significantly, to about twice the value encountered in the higher temperature experiments.

Glossary

K	*K* point (critical point of L_2 and V in a L_1–L_2–V system)
L_1	CO_2-lean liquid phase
L_2	CO_2-rich liquid phase
Q	quadruple point (coexistence of the four phases L_1–L_2–V–S)
S_1	solid *trans*-decalin
S_2	solid CO_2
UCST	upper critical solution temperature of L_1 and L_2
V	vapor phase (assumed to be pure CO_2)
$\underline{v}$	liquid-phase molar volume, mL/g-mol
$\bar{V}_i$	partial molar volume of species i (mL/g-mol
x_i	mole fraction of species i

Subscripts

nBB	*n*-butylbenzene
td	*trans*-decalin

Literature Cited

(1) Din, F., "Thermodynamic Functions of Gases", Butterworths, London, 1956, pp 102–134.
(2) Francis, A. W., *J. Phys. Chem.*, **58**, 1099 (1954).
(3) Huie, N. C., Luks, K. D., Kohn, J. P., *J. Chem. Eng. Data*, **18**, 311 (1973).
(4) Kulkarni, A. A., Zarah, B. Y., Luks, K. D., Kohn, J. P., *J. Chem. Eng. Data*, **19**, 349 (1974).
(5) Kulkarni, A. A., Luks, K. D., Kohn, J. P., *J. Chem. Eng. Data*, **19**, 349 (1974).
(6) McCaffrey, D. S., Kohn, J. P., *Chem. Eng. Prog., Symp. Ser.*, **64** (88), 22 (1968).
(7) Yang, H., Luks, K. D., Kohn, J. P., *J. Chem. Eng. Data*, **21**, 330 (1976).
(8) Zarah, B. Y., Luks, K. D., Kohn, J. P., *Chem. Eng. Prog., Symp. Ser.*, **140** (70), 91 (1974).

Received for review March 28, 1977. Accepted August 15, 1977. The apparatus used was constructed under grants from the National Science Foundation. This work was supported by National Science Foundation Grant No. GK36490X.

Activity Measurements on Liquid Thallium–Indium Alloys

B. M. Nappi, M. Pelino, D. Ferro, and V. Piacente*
Istituto di Chimica Fisica, Università di Roma, Roma, Italy

The activity of thallium in liquid In–Tl alloys in the temperature range 790–1040 K has been determined by means of vapor pressure methods. The measurements were carried out by use of a multiple rotating Knudsen source coupled with a mass spectrometer and the torsion effusion technique. The values so obtained indicate that small positive deviations from ideality exist at low temperatures.

Activity values of the elements for In–Tl alloys are not well known. The only data available concerning the liquid system are those reported by Kundys and Terpilowski (*6*) and obtained from emf measurements carried out in the temperature range 653–793 K. Apparently, no other direct determinations of the thallium activity are reported in literature. Therefore, we thought it useful to carry out some measurements of this parameter by using a multiple rotating Knudsen cell coupled with a mass spectrometer and the torsion effusion method.

Experimental Section

Samples of In–Tl alloys of eight compositions varying from 17 to 80 atom % of thallium were prepared employing spectrographic pure elements and their composition and homogenities were then checked by chemical and polarographic analysis (*8*).

The vaporization of the alloy samples was carried out by using both the mass spectrometric and the torsion effusion techniques.

Mass Spectrometry. In the mass spectrometric measurements a Bendix Time of Flight (Model 3015) mass spectrometer coupled with a multiple-rotating Knudsen cell was used. Details of the method and of the experimental procedure are reported in a previous work (*1*). The Knudsen cell has been machined from a cylindrical block of pirophyllite in which three housings have been drilled and its heating was accomplished by radiation from a tungsten filament. The temperatures were measured by using a calibrated iron–constantan thermocouple placed in the center of the block.

The In–Tl alloys were studied in five sets of vaporization experiments carried out in the temperature range 783–878 K and employing sufficient amounts of samples in order to warrant the constancy of their composition during the vaporization.

At the highest temperature, Tl^+ was the only ion species observed in the mass spectrum and, therefore, the variation of its intensity with the temperature was measured over the temperature range explored. The log I^+T vs. $1/T$ points were then treated by the least-squares method, and the relative constants of the ion intensity–temperature equations so derived are reported in Table I. The measured ion intensity values have been corrected for the calibration factors, γ_1, which account for the

0021-9568/78/1723-0047$01.00/0 © 1978 American Chemical Society

Table I. Ion Intensity Values as a Function of Temperature for Various Compositions in the Tl-In System Measured during the Mass Spectrometric Investigations

Run	Housing	Composition (atom % Tl)	Temp range, K	No. of points	$\log (I^+T)^a = A - B/T$	
					A	B
31.01	1	100	783-860	14	11.382 ± 0.135^b	8550 ± 150^b
	2	80			12.224 ± 0.134	8560 ± 148
	3	20			11.966 ± 0.144	8833 ± 160
31.03	1	100	785-867	14	12.256 ± 0.182	8762 ± 201
	2	63			12.298 ± 0.293	8945 ± 326
	3	39			11.894 ± 0.090	8730 ± 199
31.04	1	100	795-872	16	12.470 ± 0.172	8870 ± 112
	2	70			12.292 ± 0.118	8830 ± 130
	3	30			11.987 ± 0.137	8798 ± 151
31.06	1	100	790-870	13	12.222 ± 0.127	8665 ± 147
	2	80			12.249 ± 0.122	8754 ± 135
	3	39			11.537 ± 0.122	8439 ± 135
31.09	1	100	785-878	12	12.496 ± 0.179	8860 ± 176
	2	17			11.886 ± 0.106	8903 ± 120
	3	53			12.554 ± 0.110	9102 ± 142

[a] The ion intensity values were corrected by the calibration factor γ_i (see text). [b] All the associated errors are standard deviations.

possible differences in the geometry of the effusion holes and their nonperfect alignment during the rotation of the cell. The average values of γ_1, 1.061 ± 0.008 and 1.009 ± 0.007 for housings 2 and 3, respectively, taking as standard the housing 1 ($\gamma = 1.000$), were obtained in two determinations (runs 31.02, 31.10) made by loading the three housings with pure thallium and recording the corresponding Tl^+ intensity. In order to check the existence of thermodynamic equilibrium within the housings, pressure values of pure thallium were calculated from the measured ionic intensities by using the well-known relation $P_{Tl} = I^+_{Tl}T/K$ ($K = S\sigma\gamma = 4.1 \times 10^{-8}$; where σ is the thallium ionization cross section and γ the multiplier gain). A plot of log P vs. $1/T$ is reported in Figure 1.

The necessary instrument constant was determined by a quantitative vaporization of a known mass of pure Tl from the housing 1 (run 31.07). The second-law heat of sublimation of thallium $\Delta H_{298,s} = 42.3 \pm 0.7$ kcal/mol (average of five determinations), the third-law heat $\Delta H^\circ_{298,s} = 43.9 \pm 1.1$ kcal/mol (the necessary free-energy functions, $(G^\circ_T - H^\circ_{298})/T$, were taken from Hultgren (4)), and the selected value $\Delta H^\circ_{298} = 43.2$ kcal mol^{-1} reported by Hultgren (4) are, within the standard deviation, in agreement, and this could be considered an indication that thermodynamic equilibrium conditions actually existed within the cells.

Torsion Effusion. The apparatus used has been described in detail elsewhere (3, 7). The effusion cell was derived from a block of pyrophillite, and its geometrical constants are the following: $a_1 = (0.785 \pm 0.015) \times 10^{-2}$ cm² and $a_2 = (0.949 \pm 0.015) \times 10^{-2}$ cm² the orifice area, $d_1 = 8.4 \pm 0.5$ mm and $d_2 = 8.2 \pm 0.5$ mm their distances from the rotation axis, and $f_1 = 0.57$ and $f_2 = 0.57$ the Freeman and Searcy (2) connection factors which account for the orifice thickness.

From the cell constants and by measuring the cell deflection α, the vapor pressure P can be evaluated through the well-known relation (3)

$$P = 2K\alpha/(a_1d_1f_1 + a_2d_2f_2) \qquad (1)$$

where K is the torsion constant of the tungsten torsion filament ($K = 0.346$ dyn cm rad^{-1}) to which the cell was suspended. By using the same effusion cell for pure thallium and for its alloys, it follows that

$$a_{Tl} = \frac{P_{Tl(alloy)}}{P_{Tl(pure)}} = \frac{\alpha_{Tl(alloy)}}{\alpha_{Tl(pure)}} \qquad (2)$$

so that most of the systematic errors in the pressure measurements are eliminated in determining the activities. Alloys at the compositions 17, 30, 57, and 70 atom % of thallium were studied with this method and the results are plotted in Figure 2.

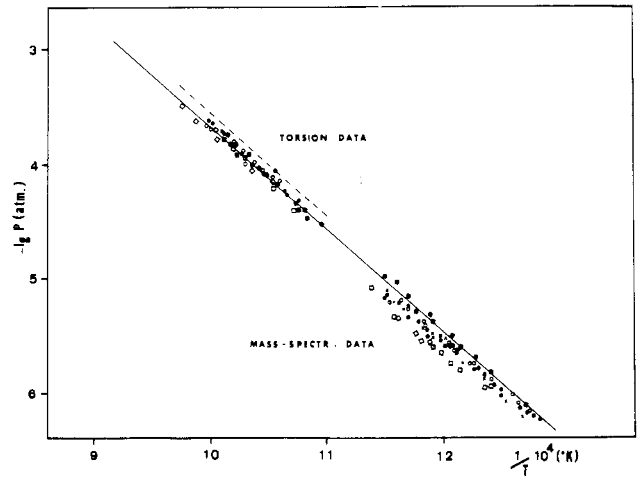

Figure 1. Vapor pressure of thallium obtained by mass spectrometric and torsion effusion techniques compared with Hultgren's data (solid line). The dotted line represents the slope obtained from torsion measured with the cell reported in Figure 5 (see text).

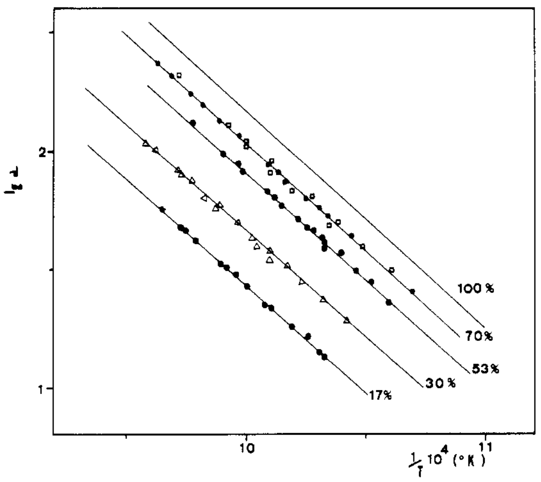

Figure 2. Plots of log α vs. $1/T$ determined by the torsion-effusion technique.

Table II. Torsion Angle of the Cell as a Function of the Temperature in the Torsion-Effusion Experiments

Run	Composition (atom % Tl)	Temp range, K	No. of points	log $\alpha = A - B/T$ A	B
22.01	100	914-983	10	11.382 ± 0.150[a]	8830 ± 142[a]
22.02	30	959-1043	17	10.724 ± 0.109	8680 ± 109
22.04	100	932-1024	11	11.143 ± 0.218	8630 ± 143
22.05	53	944-1024	18	11.000 ± 0.084	8718 ± 82
22.07	100	930-1002	15	11.724 ± 0.089	8140 ± 186
22.08	70	934-1040	12	11.178 ± 0.080	8820 ± 83
22.11	100	922-992	10	11.413 ± 0.134	8835 ± 129
22.12	17	969-1035	14	10.589 ± 0.149	8780 ± 149
22.13	70	943-1029	12	11.122 ± 0.108	8740 ± 104

[a] All the associated errors are standard deviations.

In Table II are reported the constants of the α-temperature equations in the investigated temperature range as obtained by a least-squares treatment of the experimental results. The average values of $\bar{A} = 11.316 \pm 0.180$ and $\bar{B} = 8860 \pm 200$ were used for pure thallium in the activities calculations. Also, in these measurements the thermodynamic equilibrium conditions have been checked by measuring the absolute vapor pressures of pure thallium in the experiments involving vapor pressures of pure thallium in the experiments involving the pure element and the ΔH°_{298} associated to the corresponding vaporization process. The obtained values, $\Delta H^\circ_{298,s} = 42.9 \pm 0.9$ kcal mol^{-1} (second law), and $\Delta H^\circ_{298,s} = 42.4 \pm 0.6$ kcal mol^{-1} (third law), where the errors are standard deviations, are in very good agreement with the $\Delta H^\circ_{298,s}$ value selected by Hultgren (*4*) if we consider the errors associated to the experimental measurements of the instrumental constants and to the determination of the torsion angle and the temperature of the cell. At the end of each experiment it was verified that the variation of the composition of the alloy samples considered is negligible (~0.5 atom % of thallium). Since the usual procedure led to a certain variation in the thallium composition when alloys at 17 atom % of Tl were analyzed, two experiments were carried out by loading the two semicells with the same amount of alloy sample, in order to measure the activity for alloys of low thallium content. Thallium was completely vaporized from samples of alloy at 17 atom % of Tl at two constant temperatures (T_1 = 1000 K and T_2 = 1074 K), and the deflection angles were determined as a function of the vaporization time while the thallium content in the alloy was decreasing.

During the vaporization carried out at the lower temperature (1000 K) some values of the variation of the angle α with the temperature were also measured at two different compositions (12.8 and 4.8 atom % of thallium). These compositions have been evaluated at the end of the vaporization considering that the area of the α vs. time plot is proportional to the weight loss of the sample according to the Knudsen equation (*5*). The measurements were carried out in a very short time interval compared to the overall time necessary for the quantitative vaporization of the sample, so that the composition remained practically constant during the measurements (see Figure 3). This fact is proved by the substantial constancy of the torsion angle at the end of each series of measurements. The values obtained with this procedure are plotted in Figure 4.

As concerns the quantitative vaporization at the temperature of 1074 K, the angles, α, measured were plotted as a function of time. From this plot, two angles at the prefixed compositions 12.8 and 4.8 atom % Tl were derived, and the values are reported in Figure 4. It is difficult to determine accurately the errors associated with the measurements, but their evaluation leads to a small uncertainty in the determination of the composition (<0.2%) and a larger uncertainty in the torsion angle (<3%).

By using the torsion technique, a further series of experiments has been carried out utilizing a particular pirophyllite cell illustrated in Figure 5. In this cell, a "semicell", can be rotated on its axis. At the beginning the two "semicells" were filled with pure thallium, and two series of determinations were carried out. In the first series carried out by using the cell in the conventional way, the dependence of α with the temperature was measured and the data so obtained are reported in Figure 6. The second series of measurements made by rotating the "semicell" has been utilized to check the calibration of the cell.

The purpose of this calibration was to verify that the two force moments operating in the cell are equal. By heating the sample

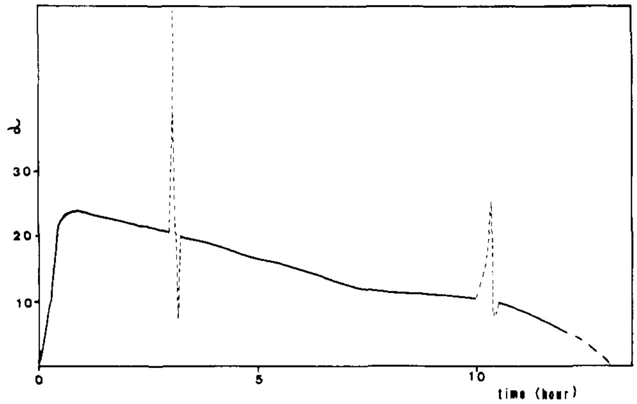

Figure 3. Plot of torsion angles vs. time measured during the quantitative vaporization of Tl at the fixed temperature of 1000 K. The dotted line represents schematically the α variations with temperature (see text).

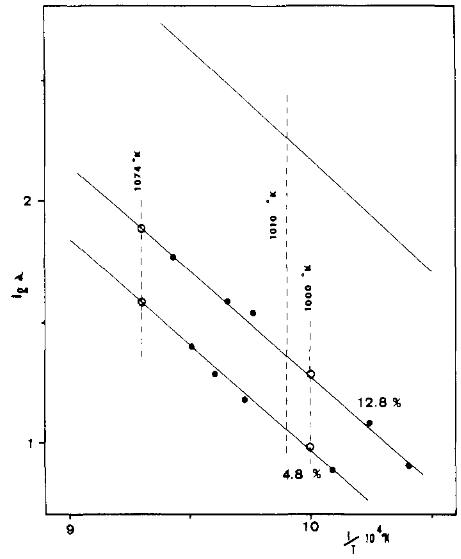

Figure 4. Plot of log α vs. $1/T$ for 12.8 and 4.8% at Tl alloys measured during the quantitative vaporizations at 1000 and 1074 K. Points (●) were measured during the quantitative vaporization at 1000 K (see text).

Table III. Torsion Angles of the Cell as Function of the Temperature Measured with the Cell Illustrated in Figure 5

Cell A	Cell B	Effusion hole position of cell B	ΔT, K	$\log \alpha = A - B/T$ A	B
Tl pure	Tl pure	Conventional	885–1002	10.958 ± 0.074^a	8928 ± 73^a
Tl pure	70% at Tl	Same as cell B	964–1078	9.460 ± 0.243	8410 ± 240
Tl pure	53% at Tl	Same as cell A	964–1067	9.864 ± 0.309	8461 ± 314
Tl pure	30% at Tl	Same as cell A	936–1063	10.204 ± 0.173	8664 ± 170

[a] Average of two experiments.

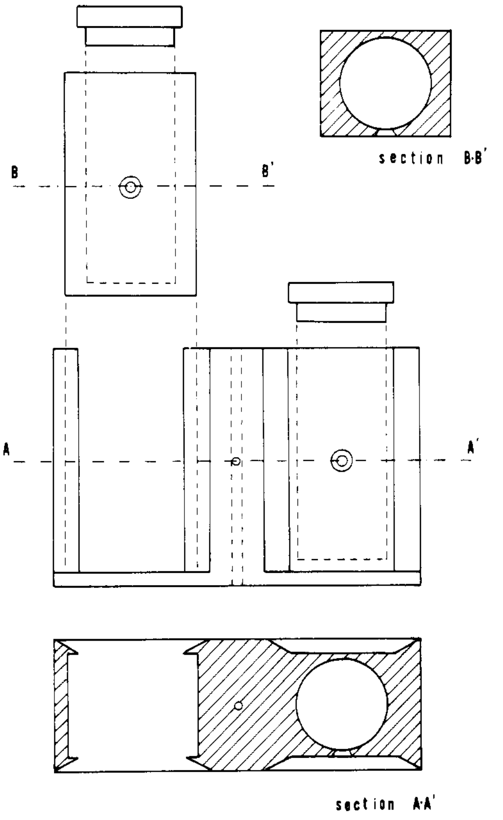

Figure 5. Schematic diagram of the torsion effusion cell.

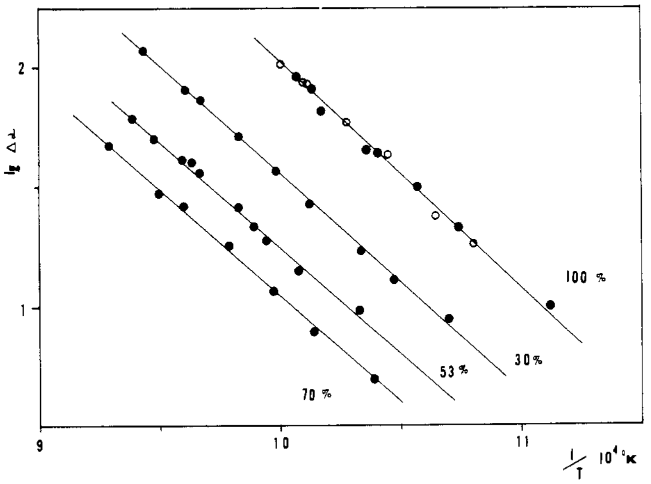

Figure 6. Plots of log α for pure thallium and log $\Delta\alpha$ for In–Tl alloys vs. 1/T measured by employing the cell reported in Figure 5.

to 1100 K, it was observed that the torsion angle was practically null ($\alpha = 2°$) and this fact shows also that the cell is negligibly removed from the original balance position when the two forces operate in the same direction.

Table IV. Activity and Partial Molar Free Energy Values of In and Tl in Liquid Alloys at 920 K

N_{Tl}	a_{Tl}	a_{In}	$-\Delta\bar{G}_{Tl}$, cal/g-atom	$-\Delta\bar{G}_{In}$, cal/g-atom	$-\Delta G_{tot}$, cal/g-atom
0.1	0.14	0.90	3594	193	533
0.2	0.27	0.81	2393	385	787
0.3	0.39	0.71	1721	626	954
0.4	0.51	0.62	1231	874	1017
0.5	0.61	0.54	904	1126	1015
0.6	0.70	0.45	652	1460	975
0.7	0.78	0.37	454	1818	863
0.8	0.85	0.28	297	2327	703
0.9	0.92	0.18	152	3135	451

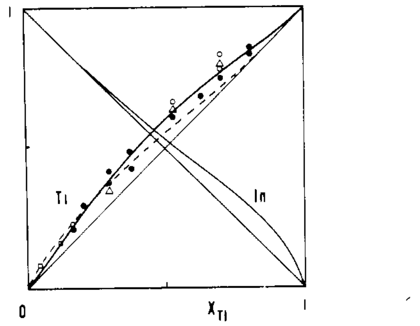

Figure 7. Thallium and indium activities in liquid alloys: (●) mass spectrometric data (830 K); (○) torsion data (1010 K); (□) torsion data obtained during the quantitative vaporizations (1010 K); (△) torsion data obtained by using the cell reported in Figure 5 (1010 K). (—)The solid line represent the proposed data at the average temperature of 920 K; (- - -) the dotted line represents the Kundy and Terpilowski results (723 K).

After this calibration run, the alloys to be studied were placed in the "semicell" and $\Delta\alpha$ values were measured at different cell temperatures. The experimental data were treated by the least-squares method and the results summarized in Table III and plotted in Figure 6.

The use of this cell could be considered alternative to the use of the conventional one in the study of alloys as it allows one to measure activities at temperatures where the high vapor pressure of one of the elements makes the conventional technique much too sensitive toward torsion angle measurements.

Results and Discussion

The thallium activities in In–Tl alloys of different compositions have been calculated at the average temperature of 830 K from the mass spectrometric data and at 1010 K from the torsion-effusion data. By using the equations reported in Tables I and II, the activity values were evaluated through the relation

$$a_x = \exp(A_x - B_x/T)/\exp(A^0 - B^0/T) \tag{3}$$

where A^0, A_x, B^0, and B_x are the constants reported in Tables I and II, respectively, for pure thallium and thallium alloyed at composition x. The values so obtained are plotted in Figure 7. In the same figure are also reported the activity values at 12.8

and 4.8 atom % of Tl obtained during the vaporization and estimated at the same temperature of 1010 K directly from the slopes reported in Figure 4.

From the $\Delta\alpha$ values measured with the cell illustrated in Figure 5 the activity values of the analized alloys are derived using the relation

$$a = 1 - 2[\exp(A_x' - B_x'/T)/\exp(A_0' - B_0'/T)] \quad (4)$$

where the A_x', B_x', A_0', and B_0' are the constants reported in Table III. The values obtained with this procedure are also reported in Figure 6.

In agreement with Kundys and Terpilowsky's activity data measured at 723 K from emf measurements (*6*), the results here obtained show that the In–Tl solution has a quasi-ideal behavior with a small positive deviation.

This quasi-ideal behavior is not surprising if one considers that the differences in the atomic radii and in the electronegativity of thallium and indium are very small (*9*).

As the activity values derived from both mass spectrometric and torsion–effusion measurements at 830 and 1010 K are comparable within the reported errors, we have chosen the midrange temperature, 920 K, to derive the activities and the free energy of mixing for both elements in the different alloys.

The activity of indium has been derived in the usual way by a graphical integration of the Gibbs–Duhem equation (*10*). The β values $\beta = \ln \gamma_{Tl}/(1 - N_{Tl})^2$ necessary for this integration were evaluated for the investigated alloys by using the relation

$$\beta = [(A_x - A_0) - (B_x - B_0)/T](1 - N_{Tl})^{-2} \quad (5)$$

The activity values of both components so calculated at 920 K and the corresponding partial molar free energies are reported in Table IV at 0.1 mole fraction intervals across the system. The mixing enthalpy of Tl can be estimated by the equation

$$\Delta H_{mix} = (1 - N_{Tl}) \int_{N_{Tl}=0}^{N_{Tl}=N_{Tl}} 4.5758(B_0 - B_x)(1 - N_{Tl})^{-2}\, dN_{Tl} \quad (6)$$

The results of these calculations, even if they are not particularly meaningful as the associated errors are greater than the ΔH_{mix} values obtained, show that the $\Delta H_{mix,s}$ are almost null and this is a further confirmation of the solution ideality.

Acknowledgments

Thanks are due to Professor F. Gauzzi for the alloy preparation, to Dr. P. Cignini for analysis of the samples, and to Professor G. Balducci for the useful suggestions in the preparation of the manuscript.

Literature Cited

(1) De Maria, G., Piacente, V., *Bull. Soc. Belg.*, **81**, 155 (1972).
(2) Freeman, R. D., Searcy, A. W., *J. Chem. Phys.*, **22**, 762 (1954).
(3) Freeman, R. D., in, "The Characterization of High Temperature Vapors", J. L. Margrave, Ed., Wiley, New York, N.Y., 1967.
(4) Hultgren, R., Orr, R. L., Kelley, K. K., "Supplement to Selected Values of Thermodynamic Properties of Metlas and Alloys", Department of Mineral Technology, University of California, 1967.
(5) Knudsen, M., *Ann. Phys. (Leipzig)*, **28**, 75 (1909).
(6) Kundys, E., Terpilowski, J., *Arch. Hutn.*, **9**, 333 (1964).
(7) Piacente, V., DeMaria, G., *Ric. Sci.*, **39**, 549 (1969).
(8) Pribil, R., Zabransky, Z., *Collect. Czech. Chem. Commun.*, **16**, 554 (1951).
(9) Samsonov, G. V., "Handbook of the Physicochemical Properties of the Elements", English Translation, IFI Plenum, New York, N.Y., 1968.
(10) Wagner, C., "Thermodynamics of Alloys", Addison-Wesley, London, 1952, p 16.

Received for review March 14, 1977. Accepted September 20, 1977. The research has been sponsored by the Consiglio Nazionale delle Ricerche through "Centro di Termodinamica Chimica alle Alte Temperature" C.N.R.—Roma.

Some Data on Phase Equilibria in the System Benzene–$FeCl_3$–H_2O–HCl at 20 °C

Henk van den Berg*
Chemical Engineering Laboratory, State University of Groningen, Groningen, The Netherlands

The solubility of iron trichloride in benzene (B) as a function of the water content of benzene has been determined quantitatively. At all values of the molar ratio $FeCl_3$:B a good solubility is guaranteed if the ratio H_2O:$FeCl_3$ in the mixture of $FeCl_3$, H_2O, and benzene amounts to 1. Maximum solubility (in the form of the $FeCl_3$–H_2O complex) amounts to 0.075 M at a HCl concentration of 0.02 M. By the addition of HCl up to a concentration of 0.70 M, this solubility increased to 0.10 M. The solubility in dry benzene and the solubility of the higher hydrates are comparatively small.

This study on the phase equilibria of B–$FeCl_3$–H_2O–HCl (B = benzene) was carried out to contribute to a better insight into the industrial process of the chlorination of benzene. The coordinative conclusions on phase equilibrium data, on kinetics measured in a homogeneous liquid mixture of the reactants, and on chlorinations carried out in a bubble column have been collected (*2*, *3*). In orientating experiments we found that the solubility of iron trichloride depends strongly on the water content of the medium. To determine quantitatively the solubility of iron trichloride as a function of the water content of the system, we carried out the following experiments.

Experimental Section

We prepared heterogeneous systems of iron trichloride and H_2O in 250 mL of B with overall compositions lying between the successive hydrates: thus between 0 and 2, 2 and 2.5, 2.5 and 3.5, 3.5 and 6 hydrate. The existence of these hydrates has been measured by Bakhuis Roozeboom (*1*, *6*). These mixtures were obtained by addition of anhydrous $FeCl_3$ and $FeCl_3 \cdot 6H_2O$ (U.C.B., tout pure) or by addition of anhydrous $FeCl_3$ and H_2O to benzene. In all these experiments so much iron trichloride is added that a precipitate is formed. In some experiments a gentle stream of HCl gas, dried on a molecular sieve, was bubbled through the mixture for 25 min. All mixtures were magnetically stirred. After the precipitate had settled we took samples of the liquid. We then

---

* To whom correspondence should be addressed at Dow Chemical (Nederland) B.V., P.O. Box 48, Terneuzen, The Netherlands.

© 1978 American Chemical Society